Journal of Physiology (1992), **457**, *pp.* 229–246
With 10 figures
Printed in Great Britain

EXPRESSION AND CHARACTERIZATION OF A CANINE HIPPOCAMPAL INWARDLY RECTIFYING K^+ CURRENT IN *XENOPUS* OOCYTES

BY J. CUI*, G. MANDEL†, D. DIFRANCESCO‡, R. P. KLINE§, P. PENNEFATHER‖, N. B. DATYNER*, H. C. HASPEL* AND I. S. COHEN*¶

*From the *Department of Physiology and Biophysics, Health Sciences Center and the †Department of Neurobiology and Behavior, SUNY, Stony Brook, NY 11794, USA, ‡Dipartimento di Fisologia e Biochimica Generali, via Celoria 26, 20133 Milano, Italy, the §Department of Pharmacology, College of Physicians and Surgeons, Columbia University, 630 West 168th Street, New York, NY 10032, USA and the ‖Faculty of Pharmacy, University of Toronto, Toronto, Ontario, Canada, M5S 2S2*

(*Received 13 December 1991*)

SUMMARY

1. An inwardly rectifying potassium current expressed in *Xenopus laevis* oocytes injected with canine hippocampal poly(A)$^+$ RNA was investigated with the two-microelectrode voltage clamp technique.

2. *Xenopus* oocytes injected with canine hippocampal poly(A)$^+$ RNA expressed a current activated by hyperpolarization. This current contained an instantaneous and a time-dependent component. Both components were inwardly rectifying and could be blocked by extracellular Cs^+ or Ba^{2+}.

3. The expressed current was carried mainly by K^+. Its reversal potential measured in different $[K^+]_o$s could be fitted by the Nernst equation with a slope of $-50{\cdot}7$ per tenfold change in $[K^+]_o$. Extracellular Cl^- and Na^+ made minimal contributions to the current.

4. The activation of the expressed current depended on both voltage and $[K^+]_o$. Activation started near E_K and the activation curve shifted along the voltage axis in parallel with E_K when $[K^+]_o$ was altered.

5. The activation time constants of the expressed current also depended on both voltage and $[K^+]_o$. The voltage dependence of the time constants was bell-shaped and the peak value was at a potential 30–50 mV more negative than E_K. The voltage dependence of the time constants shifted along the voltage axis when E_K was changed.

6. The poly(A)$^+$ RNA extracted from canine hippocampus was fractionated in a 10–31% linear sucrose gradient. The size of the mRNA required to express the inwardly rectifying current was estimated to be around 4 kb.

7. In conclusion, the expressed current is an inwardly rectifying potassium current. The canine hippocampal mRNA should be an excellent source for expression-cloning of the inward rectifier channel.

¶ To whom correspondence should be addressed.

MS 9966

INTRODUCTION

The inward rectifier is a voltage-dependent ion channel which allows K^+ to move in more easily than out across the cell membrane. Inward (anomalous) rectification was first described by Katz (1949) in the frog skeletal muscle fibre and was then found in cardiac cells (Noble, 1965) and egg cells of starfish (Hagiwara & Takahashi, 1974) and tunicates (Ohmori, 1978). Inward rectifiers in these preparations have been extensively studied (Adrian, 1969; Hagiwara, Miyazaki & Rosenthal, 1976; Standen & Stanfield, 1979; Sakmann & Trube, 1984; Kurachi, 1985; Cohen, DiFrancesco, Mulrine & Pennefather, 1989; Pennefather, Oliva & Mulrine, 1992). They share many properties which can be considered characteristic of an inward rectifier (Thompson & Aldrich, 1980; Hagiwara, 1983; Hille, 1984; Gintant, Cohen, Datyner & Kline, 1991): (1) they are activated on hyperpolarization and can be blocked by external Cs^+ or Ba^{2+}; (2) the currents can have both an instantaneous and a time-dependent activation; (3) the activation of the currents depends on both the voltage and the extracellular $[K^+]$, its activation curve shifts along the voltage axis in parallel with E_K. The major function of inward rectifiers is to maintain the resting membrane potential.

Inwardly rectifying potassium currents have also been described in many nerve cells, in both invertebrates (Kandel & Tauc, 1966) and vertebrates (Constanti & Galvan, 1983; Williams, North & Tokimasa, 1988). Recently an inward rectifying current in CA1 neurons of rat hippocampus was also reported (Grove & Halliwell, 1990).

Xenopus oocytes as a heterologous expression system have been used successfully as a functional assay to clone neurotransmitter receptors (Masu, Nakayama, Tamaki, Harada, Kuno & Nakanishi, 1987; Hollmann, O'Shea-Greenfield, Rogers & Heinemann, 1989) and ion channels (Frech, VanDongen, Schuster, Brown & Joho, 1989; Jentsch, Steinmeyer & Schwarz, 1990). They have also been used extensively to study ion channel properties (Krafte, Goldin, Auld, Dunn, Davidson & Lester, 1990) and the structure–function relationship of channel molecules (Hoshi, Zagotta & Aldrich, 1990; Isacoff, Jan & Jan, 1991; Singer, Biel, Lotan, Flockerzi, Hofmann & Dascal, 1991). The recent studies of potassium channels have greatly improved our understanding of both the gating and permeation characteristics of these types of ion channels (for review see Miller, 1991). However, to our knowledge the cation channels cloned to date are all depolarization activated. The inward rectifier is activated on hyperpolarization. Cloning this channel and studying its structure–function relationship would shed light on another mechanism for gating of ion channels.

We report here the functional expression of an inwardly rectifying potassium current in *Xenopus* oocytes microinjected with mRNA prepared from canine hippocampus. As the first step toward the cloning of the inward rectifier and studying its structure–function relationship, the ion selectivity and gating properties of this expressed current were characterized. The mRNA was fractionated and the size of the mRNA required for the expression of this channel was also determined. Part of these results have been presented to the 1992 meeting of the American Biophysical Society (Cui, Mandel, DiFrancesco, Kline, Pennefather, Haspel & Cohen, 1992).

METHODS

RNA preparation. Adult mongrel dogs were anaesthetized with I.V. injection of pentobarbitone, 30 mg kg^{-1}. The brain was then rapidly removed and the hippocampus was dissected and immediately frozen in liquid nitrogen. The hippocampal tissue was then homogenized in 3 M LiCl–6 M urea and centrifuged at 10000 *g* for 90 min. The pellet was resuspended and extracted with phenol–chloroform 3 or 4 times and the final aqueous phase was ethanol precipitated (Auffray & Rougeon, 1980; Dierks, Van Ooygen, Mantei & Weissmann, 1981). Poly(A)$^+$ RNA was isolated by oligo(dT)-cellulose chromatography (Jacobson, 1987), re-precipitated with ethanol and then dissolved in sterile water.

Size fractionation of poly(A)$^+$ RNA was performed on a non-denaturing sucrose gradient according to Sumikawa, Houghton, Smith, Bell, Richards & Barnard (1982). The RNA was layered on a linear 10–31 % (w/w) gradient and was centrifuged for 17 h at 40000 r.p.m. at 2 °C in an SW41 rotor. Twenty-two fractions of approximately 0·5 ml each were collected with a UV monitor. Each fraction was ethanol precipitated and redissolved in 5 μl of sterile water.

Oocyte preparation and injection. Ovarian lobes were dissected from mature female *Xenopus laevis* that had been anaesthetized for 20–30 min in a shallow bath containing 0·2 % tricaine solution (3-aminobenzoic acid ethyl ester, Sigma). They were then treated with collagenase (2 mg/ml, Type Ia, Sigma) to remove the follicles (Dascal, Ifune, Hopkins, Snutch, Lübbert, Davidson, Simon & Lester, 1986). Stage V and VI oocytes were selected for microinjection. Fifty nanolitres of poly(A)$^+$ RNA solution (2–5 mg/ml) was injected into each oocyte with a Drummond digital microdispenser. Oocytes were then incubated at 19 °C for 2–6 days in ND96 solution (in mM: 96 NaCl, 2 KCl, 1 $MgCl_2$, 5 HEPES–NaOH, pH = 7·5) with addition of 2·5 mM pyruvate, 100 U/ml penicillin, and 100 μg/ml streptomycin.

Electrophysiology. Currents were recorded with a conventional two-electrode voltage clamp (Dagan, Minneapolis, MN 55407, USA) (Kusano, Miledi & Stinnakre, 1982). Intracellular glass microelectrodes were filled with 3 M KCl and had tip resistances between 1 and 3 MΩ. All external solutions were made up from one basic solution, which contained (in mM) 96 NaCl, 1 $MgCl_2$, 5 $MnCl_2$, 5 HEPES–NaOH, pH 7·5. In all experiments other than the ion substitution experiments the $[Na^+]_o$ was kept the same. Each concentration of KCl, CsCl, or $BaCl_2$ was obtained by addition to the basic solution. The addition of up to 120 mM KCl to the bathing solution would be expected to increase $[K^+]_i$ in our measurement of reversal potential due to the increase in solution osmolarity. In the ion substitution experiments either 80 mM NaCl or 80 mM KOH–aspartic acid was added in the basic solution. Any other changes in the external solution will be stated in the text. All recordings were obtained at room temperature (22–24 °C). The voltage clamp steps were delivered from a programmable pulse generator. The voltage and current were recorded using a PCM adaptor (VR-10, Instrutech, Elmont, NY 11003, USA) and VCR. Data were filtered at 50 Hz and analysed with the pCLAMP program (Axon Instruments, Foster City, CA 94404, USA).

RESULTS

Expression of the current

Poly(A)$^+$ RNA extracted from canine hippocampus was injected into *Xenopus laevis* oocytes. Such oocytes expressed a current that could be activated by hyperpolarization (Fig. 1*D*). This current was not found in uninjected oocytes (Fig. 1*B*) nor in the oocytes injected with RNA from other sources (data not shown). This current was blocked by extracellular Cs^+ (Fig. 1*E*) as well as Ba^{2+} (1 mM, data not shown). Cs^+ (at 1 mM) blocks the majority of this current in 40 mM $[K^+]_o$ and 10 mM Cs^+ ensured complete blockade of the current.

Figure 1*D* shows the expressed membrane currents during voltage clamp at various membrane potential levels in an RNA-injected oocyte. At hyperpolarized membrane potentials the inward currents contained two components, one instantaneous and one time dependent. Both are blocked by Cs^+ and Ba^{2+}. The time-

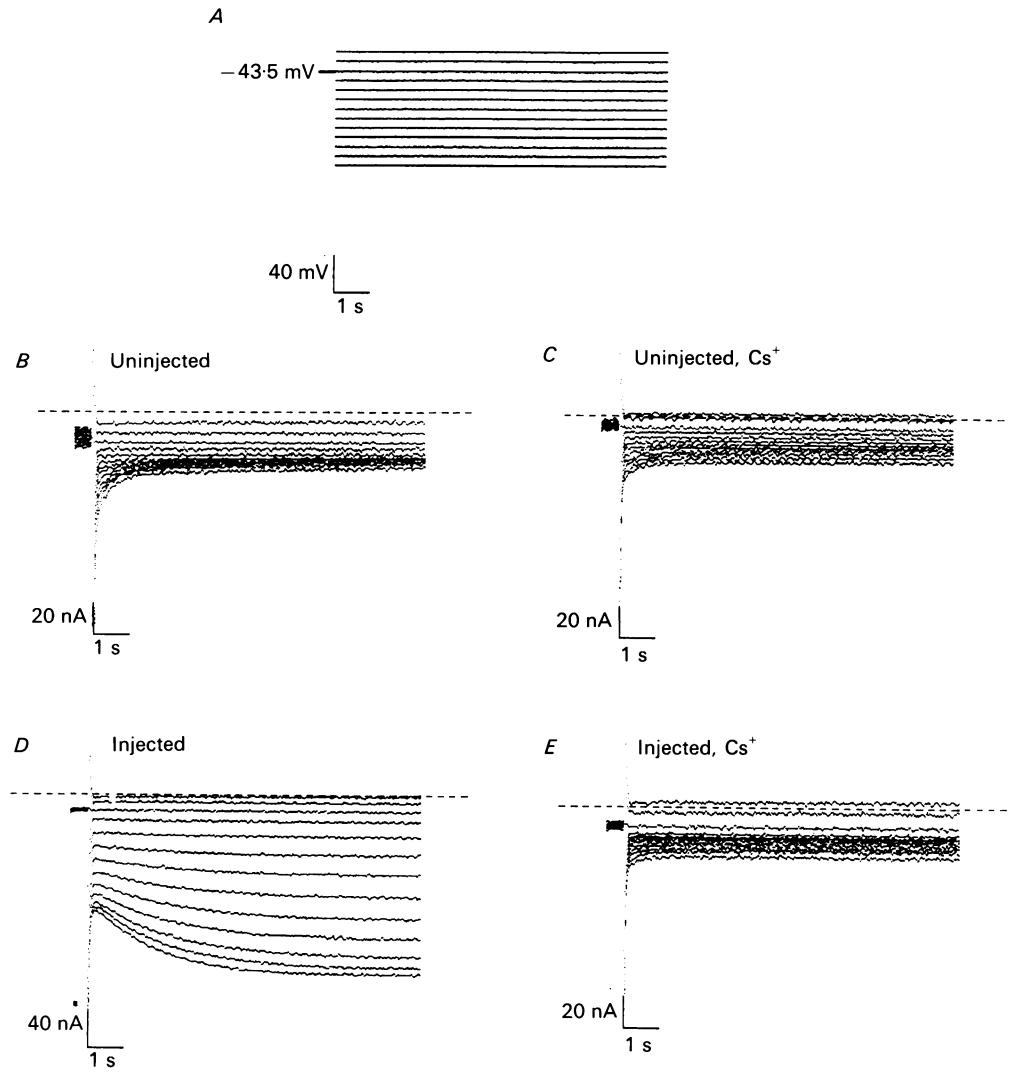

Fig. 1. Expression of a hyperpolarization-activated current in *Xenopus laevis* oocytes injected with canine hippocampal poly(A)$^+$ RNA. Note that the current scale in panel *D* is different from the others. The dashed lines in panels *B–E* show the zero current. The external solution contained 40 mM K^+. *A*, voltage protocol used in the experiments. The membrane potential was held at −43·5 mV. Voltage steps of 10 s were applied from −22·5 to −146·0 mV with an approximately −10 mV increment. *B*, current traces recorded from an uninjected oocyte. The oocyte was from the same frog as the oocyte in panels *D* and *E*, and was recorded on the same day. *C*, current traces from the same uninjected oocyte as in *B* when 10 mM Cs^+ was applied in the external solution. *D*, current traces recorded from an RNA-injected oocyte. *E*, current traces from the same RNA-injected oocyte when 10 mM Cs^+ was applied in the external solution.

dependent component could be fitted by a single-exponential function. We denote the instantaneous current and the current at steady state by I_0 and I_s, respectively. Figure 2*A* shows the current–voltage relations for these two currents. Both currents

are inwardly rectifying. The time-dependent component of the current (I_t) at steady state, $I_s - I_o$, is also inwardly rectifying (Fig. 2*B*).

The expressed current is a K^+ current

The experimental results of Fig. 2 were obtained in 40 mM $[K^+]_o$. The Cs^+-sensitive current at steady state was zero at the membrane potential of −43 mV. This zero-

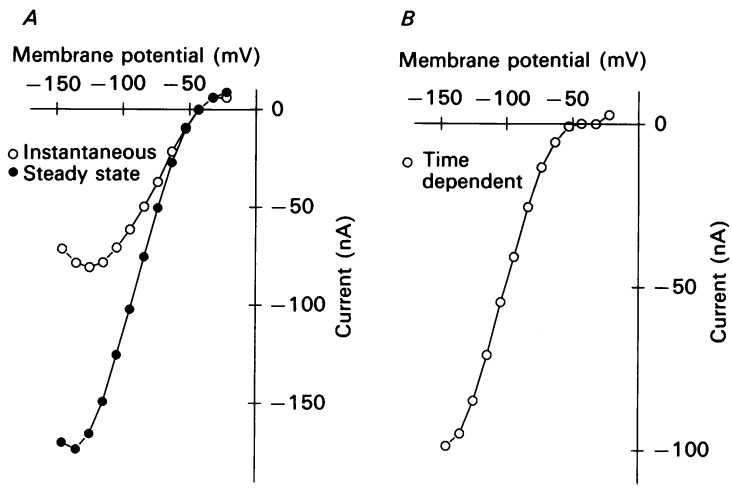

Fig. 2. The *I–V* relationship for the current expressed in an RNA-injected oocyte. The currents were elicited by the same voltage protocol as in Fig. 1*A*. The holding potential in this case was −43·2 mV. The external solution contained 40 mM K^+. *A*, the instantaneous and steady-state *I–V* curves. These curves were constructed as follows: each current trace in the solution containing 10 mM $[Cs^+]_o$ was subtracted from the current trace recorded in control solution. The Cs^+-subtracted current trace was then fitted with a single-exponential function. The instantaneous current is the current value when the exponential function was extrapolated to the beginning of the voltage step. The steady-state current is the value at infinite time. The symbols corresponding to each current are shown in the figure. *B*, the time-dependent *I–V* curve. The time-dependent current is obtained by the subtraction of the instantaneous current from the steady-state current.

current potential was not far from the calculated equilibrium potential for potassium, E_K (−32 mV), when we chose $[K^+]_i$ as 140 mM (Dascal, 1987). When the same experiment was performed in various $[K^+]_o$s, the potential where the steady-state Cs^+-sensitive current was zero tended to follow E_K. This result indicated that the expressed current might be K^+ selective.

To accurately assess the reversal potential we measured the reversal potential of the time-dependent portion of this current with a standard two-pulse protocol: The first pulse, a prepulse, was constant and hyperpolarized the oocyte sufficiently to activate a substantial time-dependent current. Following the prepulse a second pulse clamped the oocyte to a variety of test potentials. The test pulse potential at which the tail current changed direction is the reversal potential. The experimental protocol and one measurement of the reversal potential in 40 mM $[K^+]_o$ is shown in

Fig. 3*A* and *B*. In this case the reversal potential was −36·1 mV (see Fig. 3*C* for the method of measurement). We repeated this experiment with oocytes in five different $[K^+]_o$s (in mM): 10, 20, 40, 80 and 120, respectively. The results are plotted in Fig. 4. The reversal potential of this current varied almost linearly with the logarithm of

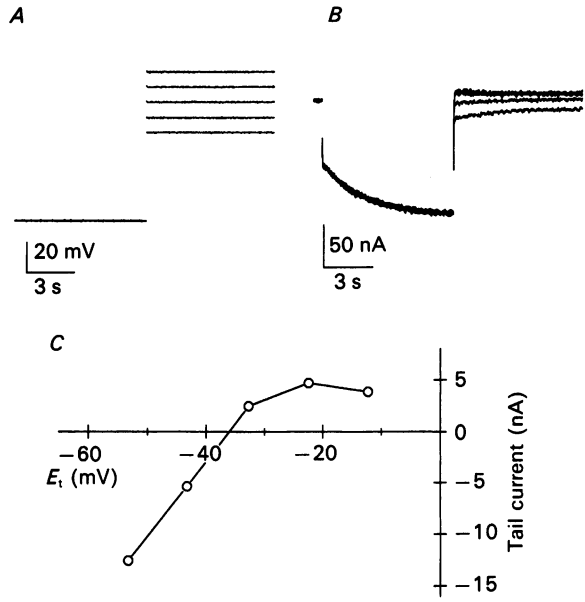

Fig. 3. Reversal potential of the expressed current. The external solution contained 40 mM K^+. *A*, the voltage protocol used in the experiment. The holding potential was −43·5 mV. The prepulse was to −114·5 mV for 8 s. The test pulses were (in mV): −12·3, −22·4, −32·8, −43·3 and −53·2, respectively; each lasted 8 s. *B*, the Cs^+-subtracted current traces. *C*, the *I–V* relationship of tail currents *versus* test potentials. Each tail current trace was fitted with a single-exponential function. The points in the figure are the magnitudes of the time-dependent tail current. The reversal potential (E_r) is where the *I–V* curve crossed the zero current line. In this case $E_r = -36{\cdot}1$ mV.

$[K^+]_o$. The straight line in Fig. 4 is the best fit of the Nernst equation. The slope of the straight line is −50·7 mV per tenfold change in $[K^+]_o$. These data provide evidence that the major ion carrier of this current is potassium.

Ion substitution experiments further demonstrated that the expressed current was a potassium current. When extracellular K^+ was substituted with Na^+ the expressed inward current totally disappeared (Fig. 5*A*). In the experiment shown in Fig. 5*A* the control solution contained 80 mM $[K^+]_o$. When the K^+ was substituted with 80 mM Na^+ the inward current decreased to the same level as if the current was blocked by Cs^+. It came back to almost the same level upon substituting K^+ back to the solution. On the other hand, when K^+ was kept the same and the extracellular Cl^- was partly substituted with non-permeant anions the expressed inward current remained the same (Fig. 5*B*). In the experiment shown in Fig. 5*B* both control and test solutions contained 80 mM $[K^+]_o$, and the test solution contained 80 mM aspartic acid substituted for 80 mM Cl^- in the control solution. The inward current was the

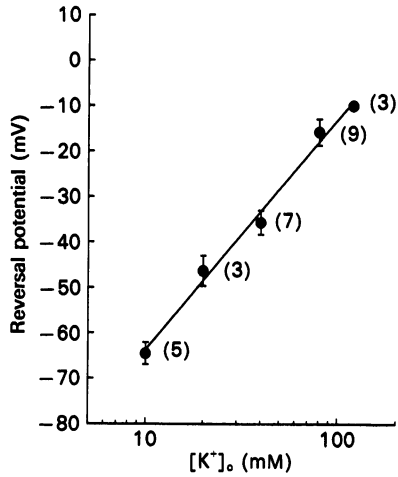

Fig. 4. The effect of $[K^+]_o$ on the reversal potential of the current expressed in the RNA-injected oocytes. The $[K^+]_o$s were (in mM): 10, 20, 40, 80 and 120 respectively. Reversal potentials were measured as described in Fig. 3 legend. Each point represents the averaged reversal potential in the corresponding $[K^+]_o$ and the numbers in parentheses are the number of oocytes measured. The error bars show the standard deviations. The straight line is the least-squares fit of the data to the Nernst equation. The slope of the line is −50·7 mV with an intersection of 180·8 mM. This intersection represents an average value since $[K^+]_i$ was presumably increased when the osmolarity of the bathing solution was increased by KCl addition (see Methods).

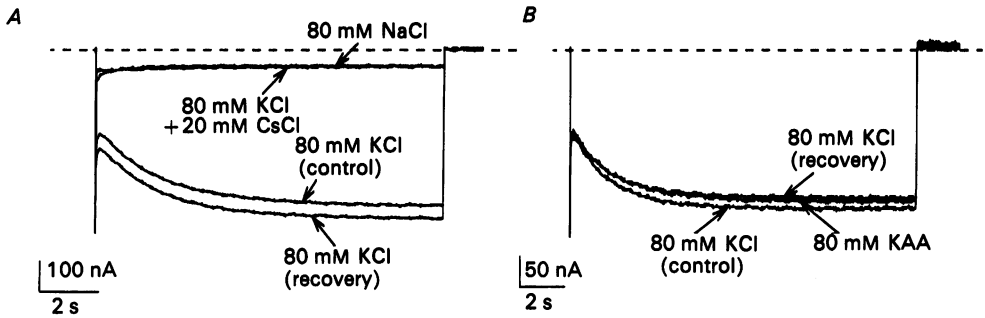

Fig. 5. Ion substitution experiments. A hyperpolarizing voltage clamp pulse was applied to the RNA-injected oocytes to activate the inwardly rectifying current in different external solutions. The solutions were described in Methods. Because a very brief sample of the holding currents prior to the pulse were captured in our record we use a dashed line in each panel to indicate their level. All current traces in each panel had the same level of holding current. *A*, 80 mM K^+ was substituted with 80 mM Na^+ and the inward current decreased to the same level obtained when the expressed current was blocked by 20 mM Cs^+. The holding potential was −20·5 mV, the voltage pulse of 12 s was to −130·5 mV. *B*, 80 mM Cl^- was substituted with 80 mM aspartic acid (AA). The inward current remained the same. The holding potential was −20·0 mV, the voltage pulse of 15 s was to −140·0 mV.

same in both solutions when the membrane potential was hyperpolarized. These results suggest that K^+ is the major ion carrier of the expressed current and Na^+ and Cl^- make minor if any contribution to it.

As described above we used the initial amplitude of deactivating current tails to estimate the reversal potential. This approach is valid only if the amplitude of each tail accurately reflects the amount of conductance, which was activated by the prepulse (i.e. no other conductance changes are occurring). We demonstrated that

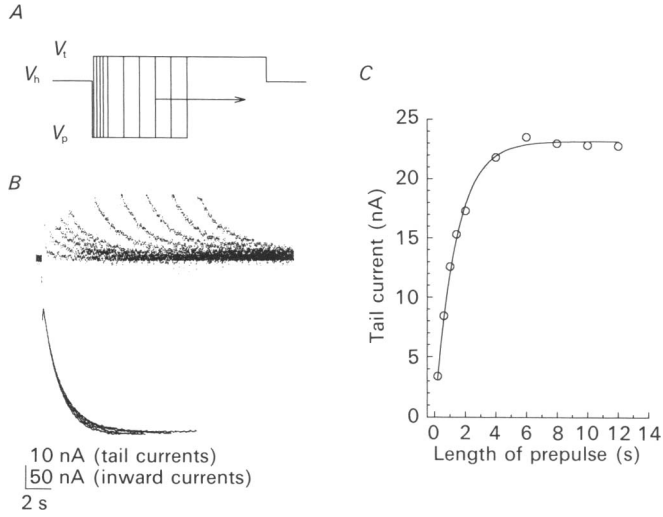

Fig. 6. Envelope test. *A*, voltage protocol for the envelope test. In the experiment shown in this figure $V_t = V_h = -0{\cdot}7$ mV, $V_p = -130{\cdot}5$ mV. $[K^+]_o$ was 80 mM. *B*, superimposed current traces. The inward currents correspond, from left to right, to V_p of duration (in s): 0·2, 0·6, 1·0, 1·4, 2·0, 4·0, 6·0, 8·0, 10·0 and 12·0, respectively. The tail currents correspond to V_t of duration 10·0 s. The deactivation time constants of the tail currents vary from 2·02 to 2·38 s, a range of less than 20%. The tail currents are scaled up to allow a better comparison with the inward currents. *C*, correlation between the time-dependent increase of the inward current during hyperpolarization and of the deactivating tail current. Each point represents the magnitude of the time-dependent tail current against the corresponding prepulse length. The continuous curve is the least-squares fit to the data points of an exponential function. The time constant of the exponential function is the measured time constant of the activating inward current elicited by the 8 s prepulse.

the tail current we measured was almost entirely the deactivating current of the expressed inward rectifier by performing the 'envelope test' (Noble & Tsien, 1969). Figure 6*A* shows the 'envelope test' protocol. A hyperpolarizing prepulse (V_p) was applied from the holding potential (V_h) for varying periods of time, between 200 ms and 12 s. Each prepulse was followed by a test pulse (V_t) of 10 s duration. The test pulse was set either positive or negative to E_K in order to obtain both outward and inward tail currents. We asked two questions. (1) Do tail current amplitudes have the same time course as the onset of the current? (2) While the tail currents grow larger, does the deactivating time course of each individual tail current remain constant? Figure 6*B* and *C* illustrates the results of this experiment obtained in 80 mM $[K^+]_o$ with a test pulse positive to E_K. The tail currents are scaled up to allow a better comparison with the inward currents during the prepulse. As shown in Fig. 6*C* the onset of the inward current and the envelope of the amplitudes of the tail currents

matched each other with the same time course. The tail currents each decline with a single-exponential time course, and the time constant of each individual tail current did not differ significantly (Fig. 6*B* and see figure legend). We repeated the 'envelope test' on a total of nineteen oocytes in three different $[K^+]_o$s (in mM: 40, 80

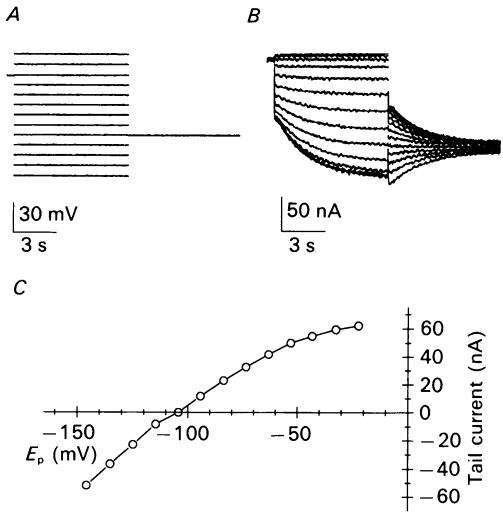

Fig. 7. Activation of the expressed current. The external solution contained 40 mM K^+. *A*, voltage protocol used in the experiment. The membrane potential was held at −43·0 mV. Prepulses of 8 s were stepped from −22·5 to −145·0 mV with about a −10 mV increment. The test pulse of 8 s following each prepulse was to −104·5 mV. *B*, Cs^+-subtracted (control−Cs^+) current traces. *C*, *I–V* relationship of tail currents plotted against prepulse voltages. The tail current was measured as described in Fig. 3 legend.

or 120) with test pulse 10, 20, 30, −10, −20, −30 or −40 mV from E_K. In general, these results supported the conclusion that our tail currents accurately reflect conductance changes of the inward rectifier and so can be used to measure its reversal potential.

The activation of the expressed current depends on $[K^+]_o$

The results described above indicate that the expressed current is an inward rectifier. A common property of inward rectifiers thus far studied is that the activation curve shifts with external potassium in parallel with E_K. We examined the activation curve for this expressed inward rectifier in the light of this previous finding. A two-pulse protocol was employed and Fig. 7*A* provides an example. The first pulse was an 8 s prepulse (E_p) to various voltages in 10 mV increments. Following the prepulse was an 8 s test pulse (E_t) to a constant voltage. Figure 7*B* and *C* provides an example of our tail current measurement in 40 mM $[K^+]_o$. In Fig. 7*B* the superimposed current records are illustrated. The tail current amplitude is plotted against the prepulse voltage in Fig. 7*C*. The tail currents had almost a linear dependence on E_p when E_p was more negative than −50 mV. When E_p was more

positive than −50 mV the amplitude of the tail currents changed less and was almost constant at E_p −20 or −30 mV, near E_K. As shown in the plot in Fig. 7*C* the activation of this current is very weakly dependent on membrane potential. The tail current did not reach saturation even when E_p was −150 mV. In other experiments

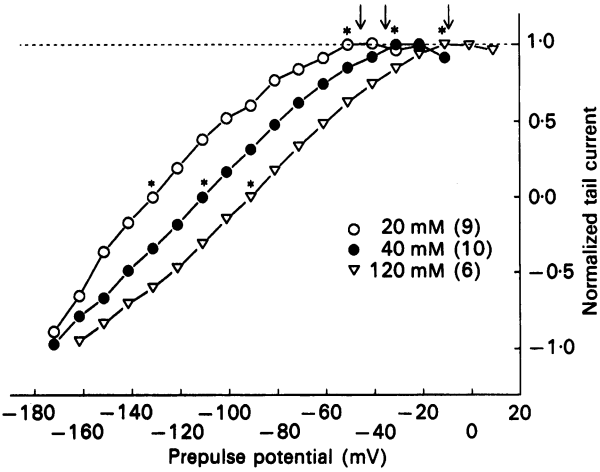

Fig. 8. The effect of $[K^+]_o$ on the activation of the current expressed in the RNA-injected oocytes. The $[K^+]_o$s were (in mM) 20, 40 and 120, respectively. The symbols corresponding to each $[K^+]_o$ are shown in the figure. The numbers in parentheses following each symbol give the numbers of experiments in the corresponding $[K^+]_o$ which were averaged to generate the curve. The arrows indicate the mean reversal potentials measured in other experiments corresponding to each $[K^+]_o$, from left to right: 20, 40 and 120 mM. Since the tail currents could not be saturated with hyperpolarization we were unable to follow the conventional normalization procedure in constructing the activation curve. In this figure we chose the tail current nearest to E_r as unity and the 9th point from it in a negative direction along the prepulse voltage axis as zero to normalize the activation curves and these points in each curve are indicated by an asterisk. The points outside the asterisks are scaled accordingly. Notice that in our experiment zero tail current was arbitrarily determined by the amplitude of the test pulse (E_t) so that this normalization procedure does not change the relative amplitude of the tail currents. However, this method forces the slope of each curve to be similar and therefore enables us to compare the starting point for activation in each $[K^+]_o$.

even at $E_p = -170$ mV the current did not demonstrate saturation. Since the oocyte membrane could not tolerate voltage steps more negative than −170 mV we were not able to obtain a complete activation curve.

We repeated the experiment with oocytes in a variety of $[K^+]_o$s. The tail currents all had similar properties to those shown in Fig. 7. To compare the activation of the current in different $[K^+]_o$s we normalized the tail currents and plotted the results obtained in three of them (in mM: 20, 40 and 120) against prepulse voltage in Fig. 8. Each curve in Fig. 8 was generated from averaged results measured in the number of different oocytes shown in the figure. The arrows in Fig. 8 indicate the E_Ks. In each $[K^+]_o$ the current starts to activate near the corresponding E_K, and the start of activation shifts along the voltage axis with changes in $[K^+]_o$. We measured similar

activation curves in 10 and 80 mM $[K^+]_o$ as well (data not shown) and the conductance started to activate near the corresponding E_K.

The time constant of activation (τ) depends on voltage and $[K^+]_o$

The time constant for activation of the expressed inward current had a bell-shaped voltage dependence (Fig. 9*A*). With increasing hyperpolarization it increased and

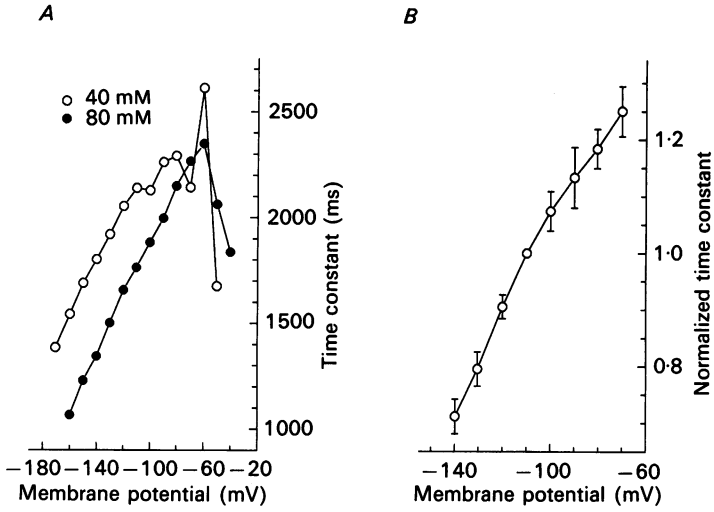

Fig. 9. The voltage and the $[K^+]_o$ dependence of the activation time constants. The voltage protocol was similar to that described in Fig. 1*A* except that in *B* the voltage pulse was 15 s in duration. *A*, the same RNA-injected oocyte was recorded in external solutions containing 40 and 80 mM K^+, respectively. Each current trace was fitted with a single-exponential function. The activation time constant of each current trace is plotted against the corresponding membrane potential. The symbols corresponding to each $[K^+]_o$ are shown in the figure. *B*, the average of normalized time constants obtained from several oocytes in 80 mM $[K^+]_o$. The error bar shows the standard deviation. The numerical data and methods used to analyse the data are shown in Table 1 and its legend.

reached a peak roughly at 30–50 mV negative to E_K, and then monotonically became briefer. Its decline after the peak was almost a linear function of the membrane potential with a less than 2-fold change for a 70 mV hyperpolarization (Fig. 9*A* and *B*). As Fig. 9*A* illustrates, the voltage dependence of the time constants shifted along the voltage axis as E_K shifted with changing $[K^+]_o$. The steepness of the voltage dependence was not altered. Table 2 provides the results from a set of experiments that compare the time constants measured in 40 and 120 mM $[K^+]_o$ with that in 80 mM $[K^+]_o$. The time constants were measured with 15 s hyperpolarizing voltage clamp pulses to several membrane potentials (in mV: −100, −110, −120 and −130). Since the time constants varied in different oocytes, we employed each oocyte as its own control and only compared τ at different $[K^+]_o$s obtained in the same oocyte. Table 2 shows the averaged ratio from five oocytes. At each membrane

TABLE 1. Voltage dependence of the time constant

E_m (mV)	Normalized time constant		No. of oocytes
	Mean	S.D.	
−140	0·71	0·03	4
−130	0·80	0·03	5
−120	0·90	0·02	6
−110	1·00	—	6
−100	1·07	0·03	6
− 90	1·13	0·05	6
− 80	1·18	0·03	6
− 70	1·25	0·04	5

The experimental conditions are decribed in the legend to Fig. 9*B*. Time constants were measured at different membrane potentials (E_m) in each oocyte. We chose the time constant at $E_m = -110$ mV as 1 and normalized time constants at other E_ms to this value for each oocyte. The normalized data were then averaged from all the oocytes and presented here and in Fig. 9*B*.

TABLE 2. External potassium dependence of the time constant (τ)

E_m (mV)	τ_{40K}/τ_{80K}		τ_{120K}/τ_{80K}	
	Mean	S.D.	Mean	S.D.
−130	1·3	0·2	0·77	0·04
−120	1·4	0·2	0·78	0·02
−110	1·3	0·2	0·80	0·05
−100	1·2	0·1	0·81	0·05

Time constants were measured at a variety of membrane potentials in three different $[K^+]_o$s (in mM: 40, 80 and 120) for each oocyte. At each membrane potential the time constants in 40 and 120 mM $[K^+]_o$ were divided by the time constant in 80 mM $[K^+]_o$. The ratios for five oocytes were then averaged.

potential the time constants had the sequence: τ(40 mM $[K^+]_o$) > τ(80 mM $[K^+]_o$) > τ(120 mM $K^+]_o$). Comparing the results provided in Table 1 and Fig. 9*B*, the difference in time constants between 40 and 80 mM $[K^+]_o$ is equivalent to a −20 to −40 mV voltage shift. Similarly the difference in time constants between 120 and 80 mM $[K^+]_o$ is equivalent to a 20–30 mV voltage shift.

Size fractionation of mRNA

Poly(A)$^+$ RNA extracted from canine hippocampus was size fractionated in a linear 10–31% sucrose gradient. Of the twenty-two fractions collected, we divided them into five groups and combined the fractions in each group. The first four groups each contained five fractions numbered from 1 to 20 and the 5th group contained fractions 21 and 22. Each group was injected into oocytes and tested for the expression of the inwardly rectifying current. Only the oocytes injected with group 4, which contained fractions 16–20, expressed the inward rectifier current. The oocytes injected with other groups had no expression of this current. We then injected each fraction from group 4 into oocytes and assayed the magnitude of the expression of this current. Figure 10 shows the results. Oocytes injected with fraction

18 had the peak expression of the inwardly rectifying current. The oocytes injected with canine hippocampal poly(A)$^+$ RNA also expressed a TTX-sensitive sodium current. In Fig. 10 we also show the expression of the sodium current in the same oocytes injected with fractionated RNA for comparison. The brain sodium channel

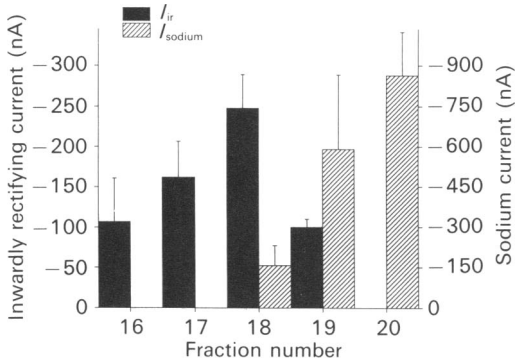

Fig. 10. Expression of inwardly rectifying potassium current (I_{ir}) and sodium current (I_{sodium}) by oocytes injected with size-fractionated canine hippocampal poly(A)$^+$ RNA. The expression of inwardly rectifying current was assayed in 40 mM $[K^+]_o$ as the difference current after addition of 10 mM Cs^+ (control − Cs^+). A hyperpolarizing voltage clamp pulse from a holding potential of −40 to −100 mV was applied for 10 s to activate the current. The Cs^+-subtracted current was plotted against the number of the fraction injected into the oocyte. The same oocytes were also assayed for the expression of sodium current in ND96 solution. The depolarizing voltage clamp pulse was from a holding potential of −100 to −10 mV for 50 ms. The peak inward current was plotted against the fraction number. Three oocytes injected with each fraction were measured and the currents averaged and then presented by the vertical columns. Error bars represent the standard deviation. From left to right the fraction has higher molecular mass mRNA species.

has an mRNA size about 7–10 kb (Noda, Ikeda, Kayano, Suzuki, Takeshima, Kurasaki, Takahashi & Numa, 1986; Goldin, Snutch, Lübbert, Dowsett, Marshall, Auld, Downey, Fritz, Lester, Dunn, Catterall & Davidson, 1986). In our experiment the oocytes injected with fraction 20 had a peak expression of this current. In another linear 10–31 % sucrose gradient run at the same time we fractionated canine hippocampal poly(A)$^-$ RNA. The 18 S and 28 S rRNA peaked at fractions 15 and 19, respectively. From these results we estimate that the size of the mRNA required to express the inwardly rectifying K^+ current is around 4 kb.

DISCUSSION

In this paper we demonstrate that *Xenopus* oocytes injected with canine hippocampal poly(A)$^+$ RNA express an inwardly rectifying potassium current. The ion selectivity and the gating properties of the current were characterized. As stated in the Introduction these characteristics of the current taken together are unique to inward rectifier channels and are shared by inward rectifiers in many other preparations.

Grove & Halliwell (1990) reported an inward rectifier in CA1 neurons of the rat

hippocampus. However, this current had a much faster activation time constant (in the range of tens of milliseconds) than that of the current reported here. To our knowledge, there have been no reports of an inward rectifier found in hippocampus with similar properties to the one we report here. The lack of a counterpart of the expressed current in the hippocampus tissue has several alternative explanations: (1) the properties of the current could be altered in *Xenopus* oocytes due to post-translational modification and a different membrane environment; (2) the localization of the channel in neurons makes it difficult to observe the current with voltage clamp measurements, or the gating properties observed were distorted; (3) the properties of the current may be species dependent, and little research has been done in canine hippocampus; (4) it has been suggested that inward rectifier channels may be a protein composed of three similar subunits (Matsuda, Matsuura & Noma, 1989; Oliva, Cohen & Pennefather, 1990). Considering that the voltage dependence of the gating properties of our expressed current was weaker than many inward rectifiers in other preparations (see below), it is possible that the expressed subunits were not correctly assembled and the current flowed through a separated subunit.

In the hippocampus there are other hyperpolarization-activated currents besides the inward rectifier currents. Halliwell & Adams (1982) reported an inward current (I_Q) carried by both K^+ and Na^+ in CA1 hippocampal neurons. I_Q was blocked by extracellular Cs^+ but was resistant to Ba^{2+}. The expressed current reported here, however, was blocked by 1 mM external Ba^{2+} (data not shown), and Na^+ made minimal contributions to it (Fig. 5*A*). The ionic selectivity and the sensitivity to Ba^{2+} distinguish this current from I_Q. Madison, Malenka & Nicoll (1986) reported a hyperpolarization-activated chloride current in hippocampal pyramidal cells. This current was not blocked by extracellular Cs^+ but was blocked by extracellular Cd^{2+}, while the current reported here was not carried by Cl^- (Fig. 5*B*) and was resistant to Cd^{2+} (data not shown) but blocked by Cs^+ (Fig. 1).

From the result of our RNA size-fractionation experiment we estimated that the molecular size range of the mRNA required for the expression of the inwardly rectifying current in oocytes was around 4 kb. This is close to the cDNA or mRNA size of many potassium channels (for instance, see Frech *et al.* 1989; Grupe, Schröter, Ruppersberg, Stocker, Drewes, Beckh & Pongs, 1990).

Properties of the expressed inwardly rectifying current

The activation time constant of our expressed current was about 2 s at a membrane potential 60 mV more negative than E_K (Fig. 9). This is slower than activation time constants of the inward rectifier in many other preparations. In cardiac myocytes (Harvey & Ten Eick, 1988), skeletal muscle (Leech & Stanfield, 1981), and neuronal preparations (Constanti & Galvan, 1983), the time constants ranged from one to tens of milliseconds. In starfish egg (Hagiwara *et al.* 1976) it was less than 0·5 s.

The activation time constant of the current was dependent on both membrane potential and $[K^+]_o$ (Fig. 9, Table 1 and 2). The voltage dependence of the time constant was bell-shaped and the peak time constants appeared at 30–50 mV more negative than E_K. In guinea-pig ventricular cells (Saigusa & Matsuda, 1988) and frog skeletal muscle (Hestrin, 1981) the activation time constant of the inward rectifier also had a bell-shaped voltage dependence. However, the peak in their preparations

appeared around E_K. Further, in most preparations the activation time constants depended on the membrane potential more steeply than in our case. For instance, in guinea-pig ventricular cells (Saigusa & Matsuda, 1988) the time constant changed e-fold with a 19·3 mV change in voltage, while in olfactory cortex neurons (Constanti & Galvan, 1983) the time constant changed e-fold with a 40 mV change in voltage.

The activation of our expressed current had a very shallow dependence on the membrane potential over at least 150 mV. The activation did not saturate even when the membrane potential was more negative than −170 mV in 80 mM $[K^+]_o$. This was unlike the inward rectifiers in other preparations where the activation usually saturated at membrane potentials 30–40 mV more negative than E_K (Ciani, Krasne, Miyazaki & Hagiwara, 1978; Leech & Stanfield, 1981; Oliva *et al.* 1990). However, in most of our experiments the inwardly rectifying current did show a saturation when the membrane potential was more negative than −120 mV (Fig. 2). This result suggests that the open-channel conductance was reduced by further hyperpolarization possibly due to open-channel blockade by an external cation as was demonstrated for several inward rectifiers (Standen & Stanfield, 1979; Harvey & Ten Eick, 1988).

Overlap of other currents

Xenopus oocytes have an endogenous Ca^{2+}-mediated chloride current ($I_{Cl(Ca)}$; Barish, 1983). This time-dependent outward current is activated by depolarization in normal solution and is due to the opening of calcium channels and consequent influx of Ca^{2+}. This current could have interfered with our tail current measurement, especially with high $[K^+]_o$. To eliminate $I_{Cl(Ca)}$ in our experiments we employed an extracellular solution containing zero calcium and 5 mM Mn^{2+} to block I_{Ca}. This chloride current was absent in our experiments.

When injected with mouse or rat brain RNA, *Xenopus* oocytes express a delayed rectifier current (Frech *et al.* 1989) or an A-type current (Christie, Adelman, Douglass & North, 1989). They both are depolarization-activated time-dependent potassium currents. However, we could not detect either of these two currents in oocytes injected with canine hippocampal poly(A)$^+$ RNA. These oocytes did, however, express a fast TTX-sensitive sodium current in addition to the inward rectifier (Fig. 10). The total time span of the sodium current was less than 50 ms and had little effect on our tail current measurements.

Conclusion

In conclusion, our analysis of the gating and selectivity of the expressed current from canine hippocampus strongly suggests it is an inwardly rectifying K^+ current. Given the size of the putative mRNA which is required for its expression and the magnitude of the expressed current, it should be an excellent candidate for expression cloning of the inward rectifier channel.

Note added in proof. Recently another inwardly rectifying K^+ current from rat basophilic leukemia cell mRNA has been expressed in *Xenopus* oocytes (Lewis, Ikeda, Aryee & Jono, 1991). The size of mRNA required for the expression of that current was also 4–5 kb, close to the size we reported here.

We would like to thank Dr James S. Trimmer for help in RNA fractionation, and Dr William Van der Kloot for helpful criticisms of the manuscript. This work was supported by grants HL20558, HL28958 and HL43731 to I.S.C.; NS22518 and a Research Grant from the Muscular Dystrophy Association to G.M.; C.N.R. AI90.00183.04 to D.D.; HL42353 to R.P.K.; the Medical Research Council of Canada to P.P., who is a Career Scientist of the Ontario Ministry of Health; and a Research Development Award from the American Diabetes Association to H.C.H.

REFERENCES

ADRIAN, R. H. (1969). Rectification in muscle membrane. *Progress in Biophysics and Molecular Biology* **19**, 339–369.

AUFFRAY, C. & ROUGEON, F. (1980). Purification of mouse immunoglobulin heavy-chain messenger RNAs from total myeloma RNA. *European Journal of Biochemistry* **107**, 303–314.

BARISH, M. E. (1983). A transient calcium-dependent chloride current in the immature *Xenopus* oocyte. *Journal of Physiology* **342**, 309–325.

CHRISTIE, M. J., ADELMAN, J. P., DOUGLASS, J. & NORTH, R. A. (1989). Expression of a cloned rat brain potassium channel in *Xenopus* oocytes. *Science* **244**, 221–224.

CIANI, S., KRASNE, S., MIYAZAKI, S. & HAGIWARA, S. (1978). A model for anomalous rectification: electrochemical-potential-dependent gating of membrane channels. *Journal of Membrane Biology* **44**, 103–134.

COHEN, I. S., DIFRANCESCO, D., MULRINE, N. K. & PENNEFATHER, P. (1989). Internal and external K^+ help gate the inward rectifier. *Biophysical Journal* **55**, 197–202.

CONSTANTI, A. & GALVAN, M. (1983). Fast inward-rectifying current accounts for anomalous rectification in olfactory cortex neurons. *Journal of Physiology* **385**, 153–178.

CUI, J., MANDEL, G., DIFRANCESO, D., KLINE, R. P., PENNEFATHER, P., HASPEL, H. C. & COHEN, I. S. (1992). Functional expression of an inwardly rectifying potassium current in *Xenopus* oocytes. *Biophysical Journal* **61**, A377.

DASCAL, N. (1987). The use of *Xenopus* oocytes for the study of ion channels. *CRC Critical Reviews of Biochemistry* **22**, 317–387.

DASCAL, N., IFUNE, C., HOPKINS, R., SNUTCH, T. P., LÜBBERT, H., DAVIDSON, N., SIMON, M. I. & LESTER, H. A. (1986). Involvement of a GTP-binding protein in mediation of serotonin and acetylcholine responses in *Xenopus* oocytes injected with rat brain messenger RNA. *Molecular Brain Research* **1**, 201–209.

DIERKS, P., VAN OOYEN, A., MANTEI, N. & WEISSMAN, C. (1981). DNA sequences preceding the rabbit β-globin gene are required for formation in mouse L cells of β-globin RNA with the correct 5′ terminus. *Proceedings of the National Academy of Sciences of the USA* **78**, 1411–1415.

FRECH, G. C., VANDONGEN, A. M. J., SCHUSTER, G., BROWN, A. M. & JOHO, R. H. (1989). A novel potassium channel with delayed rectifier properties isolated from rat brain by expression cloning. *Nature* **340**, 642–645.

GINTANT, G. A., COHEN, I. S., DATYNER, N. B. & KLINE, R. P. (1991). Time-dependent outward currents in the heart. In *The Heart and Cardiovascular System*, ed. FOZZARD, H. A., HABER, E., JENNINGS, R. B., KATZ, A. M. & MORGAN, H. E. Raven Press, New York.

GOLDIN, A. L., SNUTCH, T., LÜBBERT, H., DOWSETT, A., MARSHALL, J., AULD, V., DOWNEY, W., FRITZ, L. C., LESTER, H. A., DUNN, R., CATTERALL, W. A. & DAVIDSON, N. (1986). Messenger RNA coding for only the α subunit of the rat brain Na channel is sufficient for expression of functional channels in *Xenopus* oocytes. *Proceedings of the National Academy of Sciences of the USA* **83**, 7503–7507.

GROVE, E. A. & HALLIWELL, J. V. (1990). Two inward rectifier currents revealed in CA1 neurons of the rat hippocampus *in vitro*. *Journal of Physiology* **424**, 46*P*.

GRUPE, A., SCHRÖTER, K. H., RUPPERSBERG, J. P., STOCKER, M., DREWES, T., BECKH, S. & PONGS, O. (1990). Cloning and expression of a human voltage-gated potassium channel. A novel member of the RCK potassium channel family. *EMBO Journal* **9**, 1749–1756.

HAGIWARA, S. (1983). *Membrane Potential-dependent Ion Channels in Cell Membrane. Phylogenetic and Developmental Approaches*. Raven Press, New York.

HAGIWARA, S., MIYAZAKI, S. & ROSENTHAL, N. P. (1976). Potassium current and the effect of cesium on this current during anomalous rectification of the egg cell membrane of a starfish. *Journal of General Physiology* **67**, 621–638.

HAGIWARA, S. & TAKAHASHI, K. (1974). The anomalous rectification and cation selectivity of the membrane of a starfish egg cell. *Journal of Membrane Biology* **18**, 61–80.

HALLIWELL, J. V. & ADAMS, P. R. (1982). Voltage-clamp analysis of muscarinic excitation in hippocampal neurons. *Brain Research* **250**, 71–92.

HARVEY, R. D. & TEN EICK, R. E. (1988). Characterization of the inward-rectifying potassium current in cat ventricular myocytes. *Journal of General Physiology* **91**, 593–615.

HESTRIN, S. (1981). The interaction of potassium with the activation of anomalous rectification in frog muscle membrane. *Journal of Physiology* **317**, 497–508.

HILLE, B. (1984). *Ionic Channels of Excitable Membranes*, pp. 109–112. Sinauer Associates Inc, Massachusetts.

HOLLMANN, M., O'SHEA-GREENFIELD, A., ROGERS, S. W. & HEINEMANN, S. (1989). Cloning by functional expression of a member of the glutamate receptor family. *Nature* **342**, 643–648.

HOSHI, T., ZAGOTTA, W. N. & ALDRICH, R. W. (1990). Biophysical and molecular mechanisms of Shaker potassium channel inactivation. *Science* **250**, 533–538.

ISACOFF, E. Y., JAN, Y. N. & JAN, L. Y. (1991). Putative receptor for the cytoplasmic inactivation gate in the Shaker K^+ channel. *Nature* **353**, 86–90.

JACOBSON, A. (1987). Purification and fractionation of poly(A)$^+$ RNA. *Methods in Enzymology* **152**, 254–261.

JENTSCH, T. J., STEINMEYER, K. & SCHWARZ, G. (1990). Primary structure of *Torpedo marmorata* chloride channel isolated by expression cloning in *Xenopus* oocytes. *Nature* **348**, 510–514.

KANDEL, E. R. & TAUC, L. (1966). Anomalous rectification in the metacerebral giant cells and its consequences for synaptic transmission. *Journal of Physiology* **183**, 287–304.

KATZ, B. (1949). Les constantes électriques de la membrane du muscle. *Archives des Sciences Physiologiques* **3**, 285–299.

KRAFTE, D. S., GOLDIN, A. L., AULD, V. J., DUNN, R. J., DAVIDSON, N. & LESTER, H. A. (1990). Inactivation of cloned Na channels expressed in *Xenopus* oocytes. *Journal of General Physiology* **96**, 689–706.

KURACHI, Y. (1985). Voltage-dependent activation of the inward-rectifier potassium channel in the ventricular cell membrane of guinea-pig heart. *Journal of Physiology* **366**, 365–385.

KUSANO, K., MILEDI, R. & STINNAKRE, J. (1982). Cholinergic and catecholaminergic receptors in the *Xenopus* oocyte membrane. *Journal of Physiology* **328**, 143–170.

LEECH, C. A. & STANFIELD, P. R. (1981). Inward rectification in frog skeletal muscle fibres and its dependence on membrane potential and external potassium. *Journal of Physiology* **319**, 295–309.

LEWIS, D. L., IKEDA, S. R., ARYEE, D. & JOHO, R. H. (1991). Expression of an inwardly rectifying K^+ channel from rat basophilic leukemia cell mRNA in *Xenopus* oocytes. *FEBS Letters* **290**, 17–21.

MADISON, D. V., MALENKA, R. C. & NICOLL, R. A. (1986). Phorbol esters block a voltage-sensitive chloride current in hippocampal pyramidal cells. *Nature* **321**, 695–697.

MASU, Y., NAKAYAMA, K., TAMAKI, H., HARADA, Y., KUNO, M. & NAKANISHI, S. (1987). cDNA cloning of bovine substance-K receptor through oocyte expression system. *Nature* **329**, 836–838.

MATSUDA, H., MATSUURA, H. & NOMA, A. (1989). Triple-barrel structure of inwardly rectifying K^+ channels revealed by Cs^+ and Rb^+ block in guinea-pig heart cells. *Journal of Physiology* **413**, 139–157.

MILLER, C. (1991). 1990: *Annus mirabilis* of potassium channels. *Science* **252**, 1092–1096.

NOBLE, D. (1965). Electrical properties of cardiac muscle attributable to inward going (anomalous) rectification. *Journal of Cellular and Comparative Physiology* **66**, 127–136.

NOBLE, D. & TSIEN, R. W. (1969). Outward membrane currents activated in the plateau range of potentials in cardiac Purkinje fibres. *Journal of Physiology* **200**, 205–231.

NODA, M., IKEDA, T., KAYANO, T., SUZUKI, H., TAKESHIMA, H., KURASAKI, M., TAKAHASHI, H. & NUMA, S. (1986). Existence of distinct sodium channel messenger RNAs in rat brain. *Nature* **320**, 188–192.

OHMORI, H. (1978). Inactivation kinetics and steady-state current noise in the anomalous rectifier of tunicate egg cell membrane. *Journal of Physiology* **281**, 77–99.

OLIVA, C., COHEN, I. S. & PENNEFATHER, P. (1990). The mechanism of rectification of i_{K1} in canine Purkinje myocytes. *Journal of General Physiology* **96**, 299–318.

PENNEFATHER, P., OLIVA, C. & MULRINE, N. (1992). Origin of the potassium and voltage dependence of the cardiac inwardly rectifying K-current (I_{K1}). *Biophysical Journal* **61**, 448–462.

SAIGUSA, A. & MATSUDA, H. (1988). Outward current through the inwardly rectifying potassium channel of guinea-pig ventricular cells. *Japanese Journal of Physiology* **38**, 77–91.

SAKMANN, B. & TRUBE, G. (1984). Conductance properties of single inwardly rectifying potassium channels in ventricular cells from guinea-pig heart. *Journal of Physiology* **347**, 641–657.

SINGER, D., BIEL, M., LOTAN, I., FLOCKERZI, V., HOFMANN, F. & DASCAL, N. (1991). The roles of the subunits in the function of the calcium channel. *Science* **253**, 1553–1557.

STANDEN, N. B. & STANFIELD, P. R. (1979). Potassium depletion and sodium block of potassium currents under hyperpolarization in frog sartorius muscle. *Journal of Physiology* **294**, 497–520.

SUMIKAWA, K., HOUGHTON, M., SMITH, J. C., BELL, L., RICHARDS, B. M. & BARNARD, E. A. (1982). The molecular cloning and characterization of cDNA coding for the α subunit of the acetylcholine receptor. *Nucleic Acids Research* **10**, 5809–5822.

THOMPSON, S. H. & ALDRICH, R. W. (1980). Membrane potassium channels. In *The Cell Surface and Neuronal Function*, ed. COTMAN, C. W., POSTE, G. & NICOLSON, G. L., pp. 49–85. Elsevier/North-Holland Biomedical Press, Amsterdam.

WILLIAMS, J. T., NORTH, R. A. & TOKIMASA, T. (1988). Inward rectification of resting and opiate-activated potassium currents in rat locus coeruleus neurons. *Journal of Neuroscience* **8**, 4299–4306.